

Detection and analysis of turbulent structures using the Partial Variance of Increments method

Antonella Greco

Collaborations:

- W. H. Matthaeus, Bartol Research Institute, Delaware, USA
- K. T. Osman, University of Warwick, United Kingdom
- S. Servidio, University of Calabria, Italy
- P. Dmitruk, Universidad de Buenos Aires, Argentina
- R. D'Amicis, IFSI, Rome, Italy
- F. Valentini, University of Calabria, Italy
- S. Donato, University of Calabria, Italy

Turbulent cascade in the solar wind:
anisotropy and dissipation

18/09/2012, Meudon Observatory

Outline

- **Different interpretations of magnetic discontinuities**
- **Detection by PVI**
- **Performance of PVI:**
 - ✓ **Current sheets and magnetic reconnection in 2D MHD and Hall MHD turbulence**
 - ✓ **Current sheets and inhomogeneous kinetic effects in Vlasov turbulence**
- **Solar wind applications:**
 - ✓ **Enhanced heating in and near intermittent current sheets**
 - ✓ **Nonlinear development of MHD scale intermittency in the inner heliosphere**
- **Conclusions**

A brief overview on magnetic discontinuities

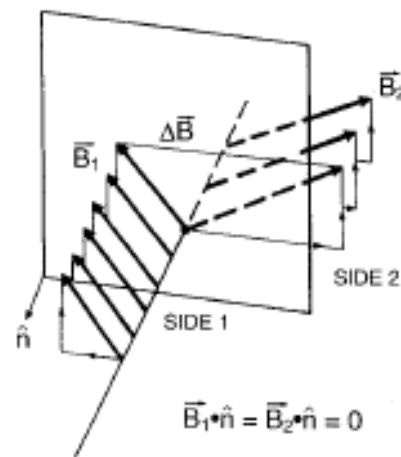
A discontinuity is an abrupt change in magnetic field vector typically defined by statistical quantities like

$$|\Delta \mathbf{b}| = |\mathbf{b}(s + \Delta s) - \mathbf{b}(s)|$$

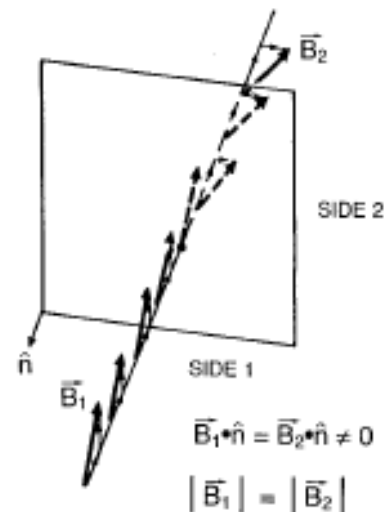
Pioneer works of *Burlaga, 1969* and *Tsurutani and Smith, 1979*

In ideal MHD, discontinuities are classified as tangential, contact, rotational, and shocks, depending on how mass, momentum and energy are transported across them

TANGENTIAL DISCONTINUITY

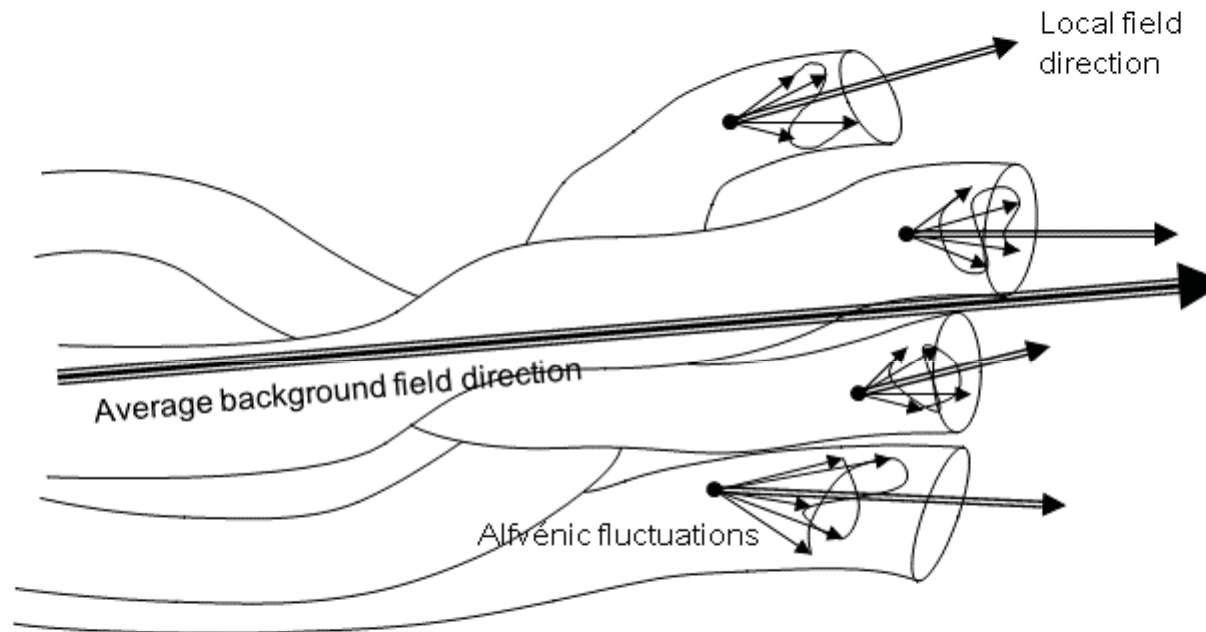


ROTATIONAL DISCONTINUITY



One interpretation of the strong discontinuities is that they are the walls between filamentary structures of a discontinuous solar wind plasma

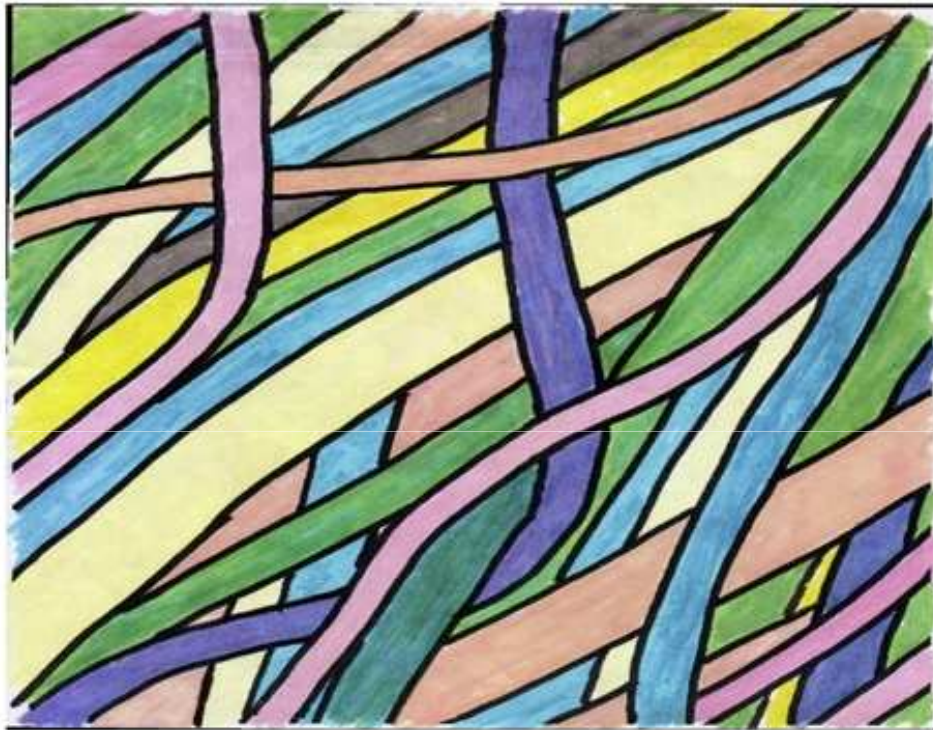
[*Burlaga, 1969; Borovsky, 2006; Borovsky and Denton, 2010*]



A sketch of the flux-tube structure of the solar-wind plasma. Plasma and magnetic-field lines are confined to individual tubes and **the walls of the tubes are solar-wind tangential discontinuities**. The magnetic-field inside a tube undergoes small angular variations from turbulence and the magnetic-field undergoes a large angular change in crossing from one tube to the next. (From *Bruno et al., 2001*).

.....while another is that some strong discontinuities are fossils from the birth of the solar wind

[*Burlaga, 1968; Marsch and Tu, 1994; Borovsky, 2008*]



A sketch of the flux tube texture of the solar-wind plasma. Each flux tube contains a different plasma and the **flux tubes move independently**. An end view (right) depicts the cross sections of the network of tubes. The scale sizes of the flux tubes correspond to the scale sizes of **granules on the solar surface**. (From *Borovsky, 2008*).

An alternative possibility is that the observed discontinuities are the current sheets that form as consequence of the broad-band cascade of magnetohydrodynamic (MHD) turbulence [*Matthaeus and Montgomery, 1980; Matthaeus and Lamkin, 1986; Carbone et al., 1990, 1995; Veltri, 1999*].

Our approach was to compare statistical properties of discontinuities, as measured using classical methods (e.g. *Tsurutani and Smith , 1979*), with intermittency properties of MHD turbulence.

First we checked this hypothesis in simulations and then, we directly compared statistical analysis from solar wind data and simulations of MHD turbulence.

We suggested that events founds in the solar wind might be of local origin as well, i.e. a by-product of the turbulent evolution of magnetic fluctuations (*Greco et al., GRL 2008, Greco et al., ApJ 2009*) and that are therefore integral to the dynamical couplings across scales.

PVI: Coherent Structure Detection

A highly reliable way to systematically find out regions of high magnetic stress and coherent structures is to identify rapid changes in the magnetic field vector calculated along a 1D path s

$$\Delta \mathbf{B}(s, \Delta s) = \mathbf{B}(s + \Delta s) - \mathbf{B}(s)$$

Employing only the sequence of magnetic increments, we compute the normalized magnitude

$$PVI = \frac{|\Delta \mathbf{B}|}{\sqrt{\langle |\Delta \mathbf{B}|^2 \rangle}} \quad \begin{aligned} \langle PVI^2 \rangle &= 1 \\ \langle PVI^4 \rangle &\text{ is related to the kurtosis} \end{aligned}$$

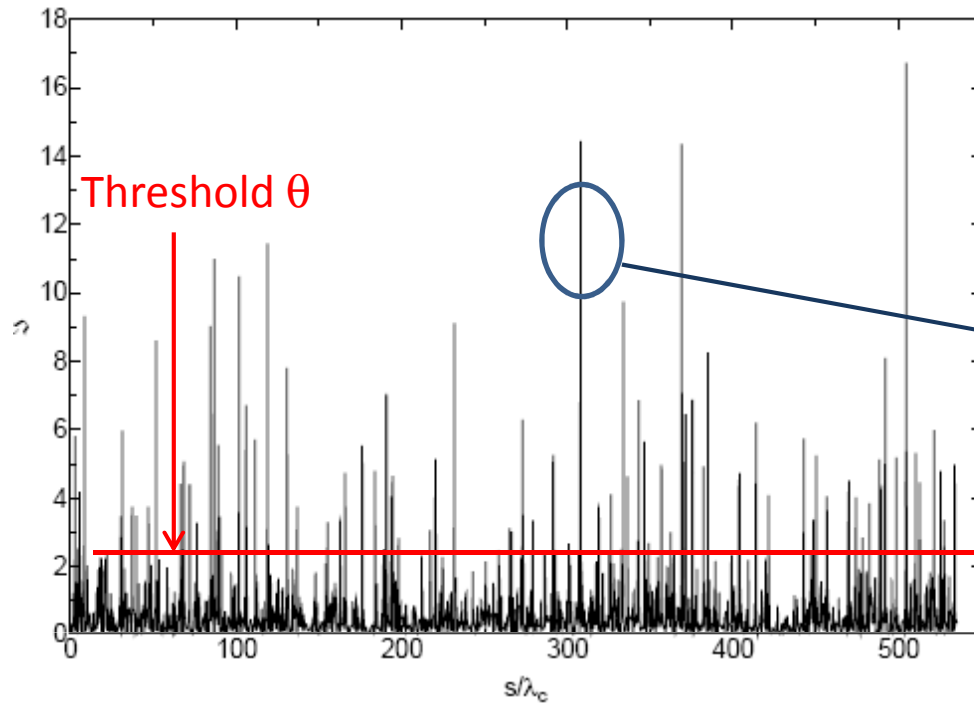
The basic idea of the PVI method is pretty simple and it is related to other measures of coherent structures, such as

Local Intermittency Measure (LIM) *Veltri et al.*, 1999, related wavelet-based techniques *Bruno et al.*, PSS 2001, Phase Coherence Index *Hada et al.*, *Vasquez et al.*, JGR 2007, *Li et al.*, ApJ 2008, *Borovsky*, PRL 2010, *Malaspina and Gosling*, JGR 2012

Some of these have in common the condition that selected parts of a data set are contributing to non-Gaussian statistics and therefore intermittency.

Scale dependent kurtosis and filtered kurtosis provide complementary global information about non-Gaussianity at different scales.

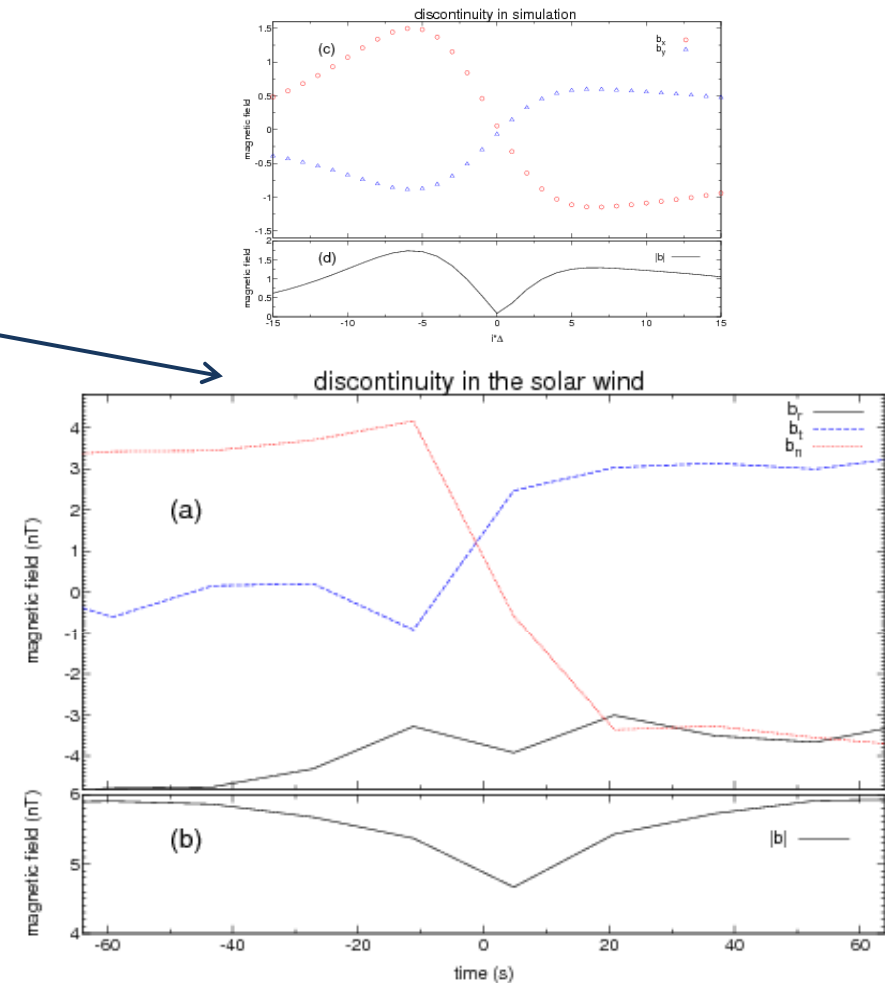
How to select these structures?



The signal below the threshold is Gaussian distributed

**For each threshold θ ,
a number of discontinuities
can be localized and “counted”**

Larger PVI \rightarrow more strongly discontinuities



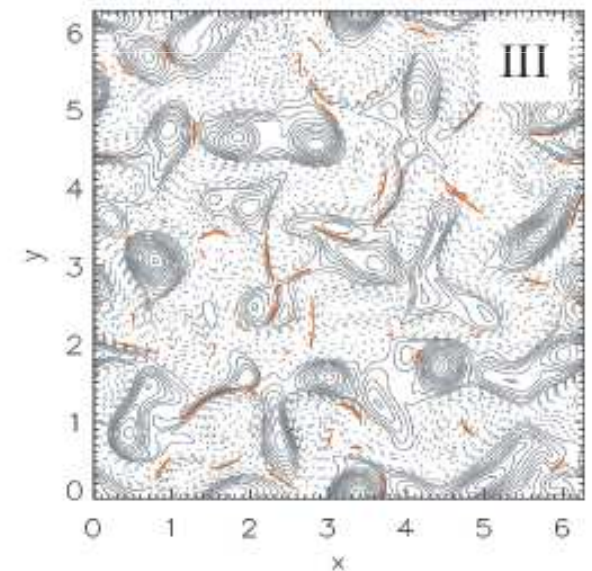
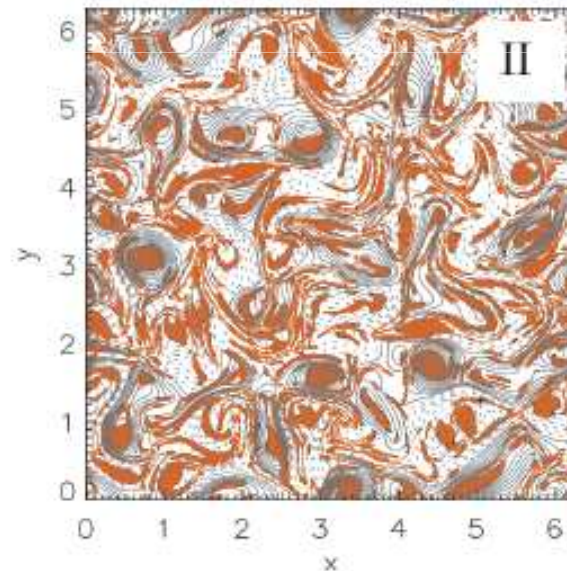
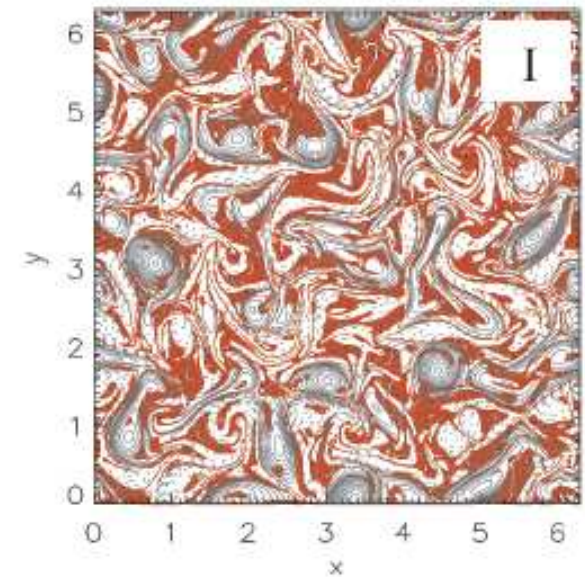
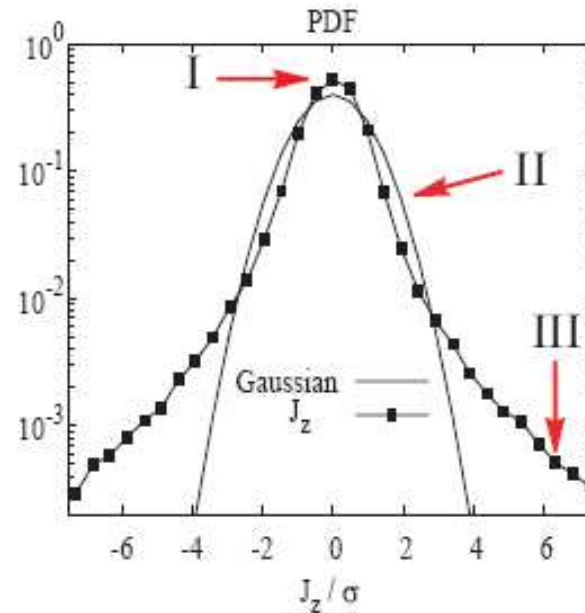
Typical tangential discontinuity signatures: rotation of the magnetic field followed by a depression of the magnitude of **b**.

We numerically select points that contribute to each band, and produce an image consisting of those points. We superpose this image with a plot of magnetic field lines in the x-y plane.

Region III : small scale current sheet-like structures that form the sharp boundaries between the vortices

Region II : current cores that populate the central regions of the magnetic islands (Sorriso'talk on Monday afternoon)

Region I: low values of fluctuations that lie mainly in the lanes between magnetic islands



Real space-picture of intermittency

contours of constant magnetic potential A_z :

$A_z > 0$ solid, $A_z < 0$ dashed

Greco *et al.*, ApJL, 2009

Statistical association between discontinuities and reconnection

Such small scale structures are candidates to be active sites of magnetic reconnection. Indeed, reconnection locally occurs relatively frequently at these thin current sheets (*Matthaeus and Montgomery, 1980; Sundkvist et al., 2007; Servidio et al., 2009-2010*).

If one identifies a current sheet in turbulence, how likely is it to be also an active reconnection site?

To do this, we combined approaches, recently developed in studies of discontinuities (*Greco et al., 2008 and 2009*) and reconnection in turbulence (*Servidio et al., 2009 and 2010*), in order to identify reconnection events within a set of identified current sheets

Once that a collection of events which are likely to be reconnection sites are identified, one can look for detailed signatures as a subsequent step

A link with Local reconnection

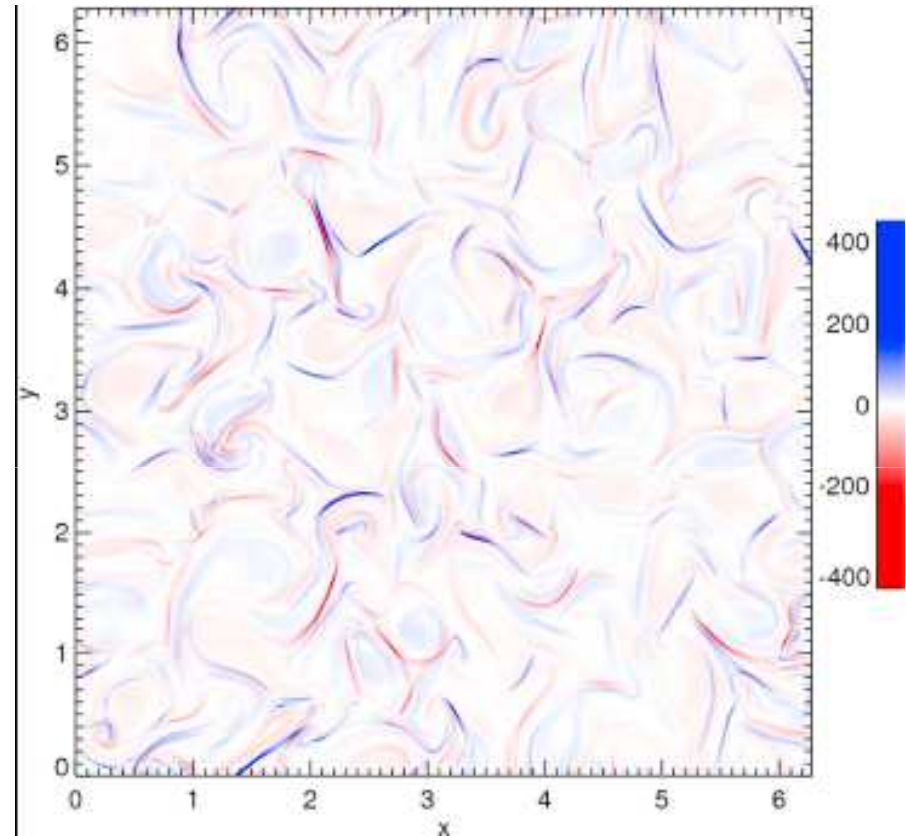
2D MHD simulation with 4096^2 grid points

$R_\nu = R_\mu \sim 2000$

Correlation length $\lambda_c = 1.8 \times 10^{-1}$

Dissipation length $\lambda_d = 4.6 \times 10^{-3}$

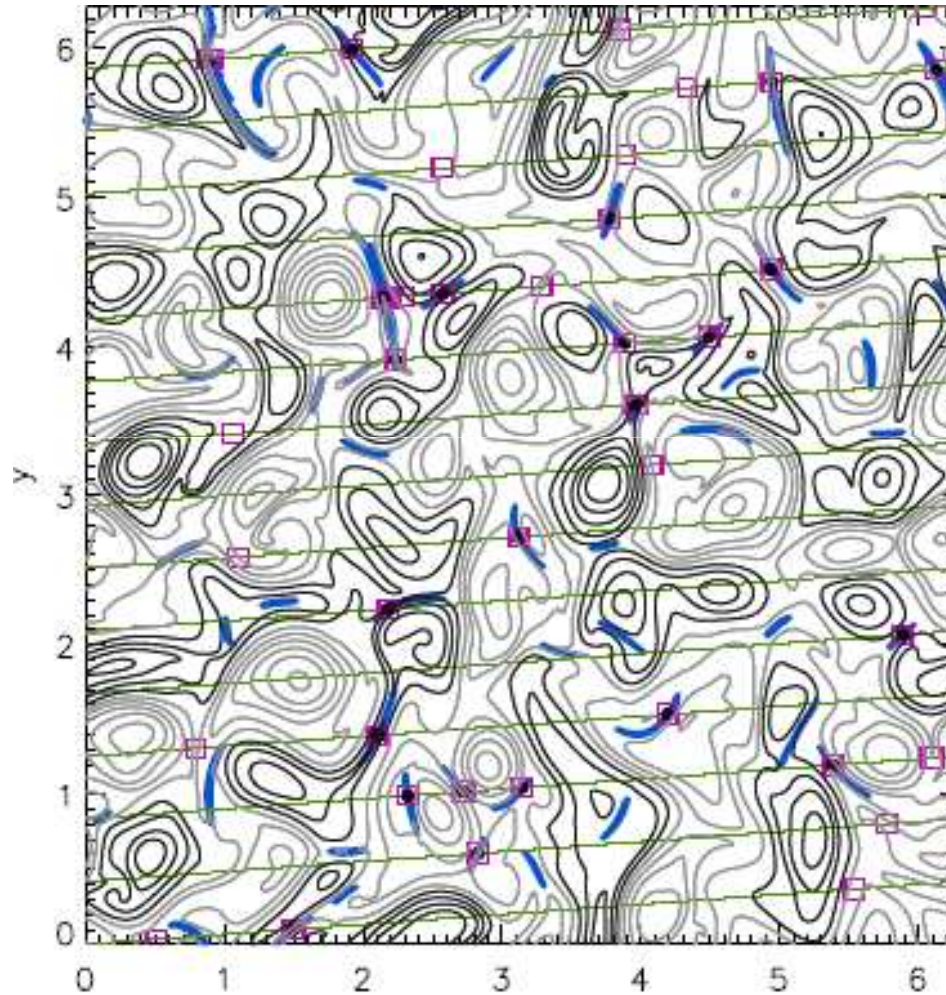
When turbulence is fully developed, magnetic islands appear and between them, the perpendicular component of j becomes very high.



These thin current structures are not present in the random-phase initial data

An Example of the location of discontinuities along the path with $\theta=5$

We adopt a spacecraft – like sampling and we fix our attention on the structures it samples



Contour lines of the magnetic field.

Strong current regions around \mathbf{x} points (blue) identified with a cellular automata technique [Servidio *et al.*, PRL 2009].

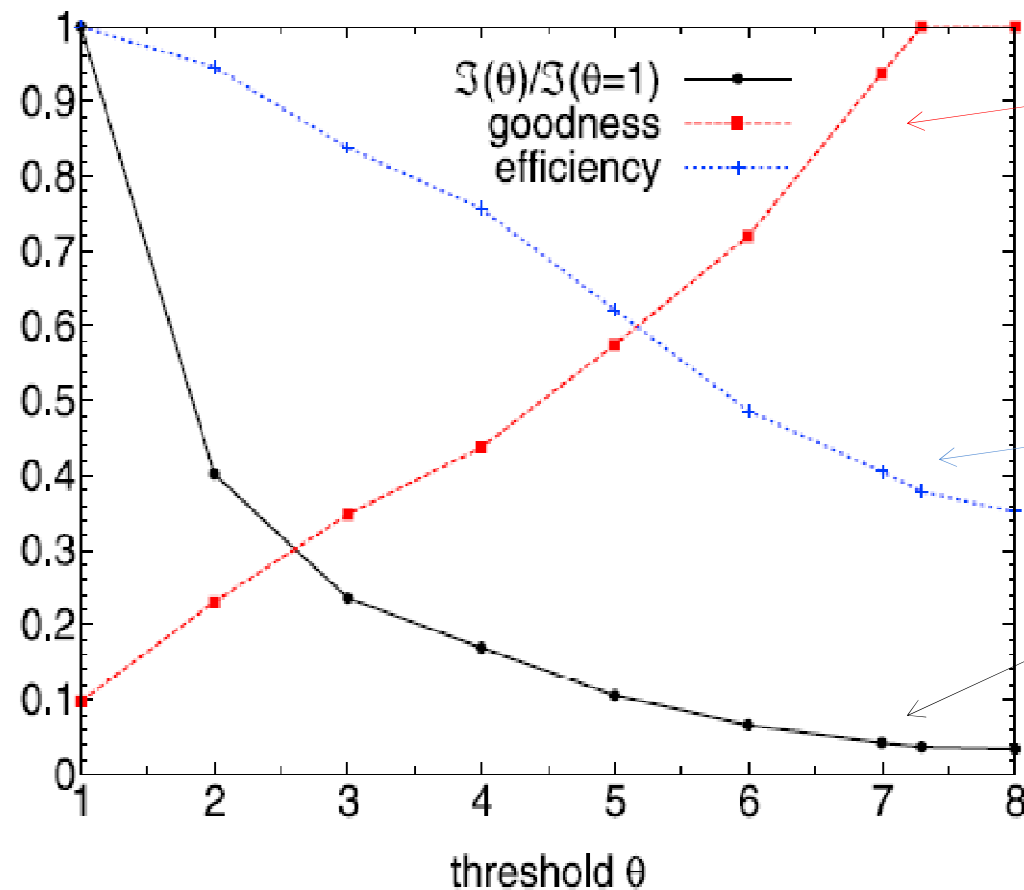
The discontinuities identified by PVI technique with a threshold $\theta = 5$ (open magenta squares \square).

Black bullets \bullet are TDs which correspond to RZ

Some TDs are not RZs!

There is an *association*, not an identity, between TDs and the encounters of the trajectory with the reconnection regions

■ Discontinuities & Reconnection



#reconnection events/
#discontinuities

For high thresholds
→ 100%

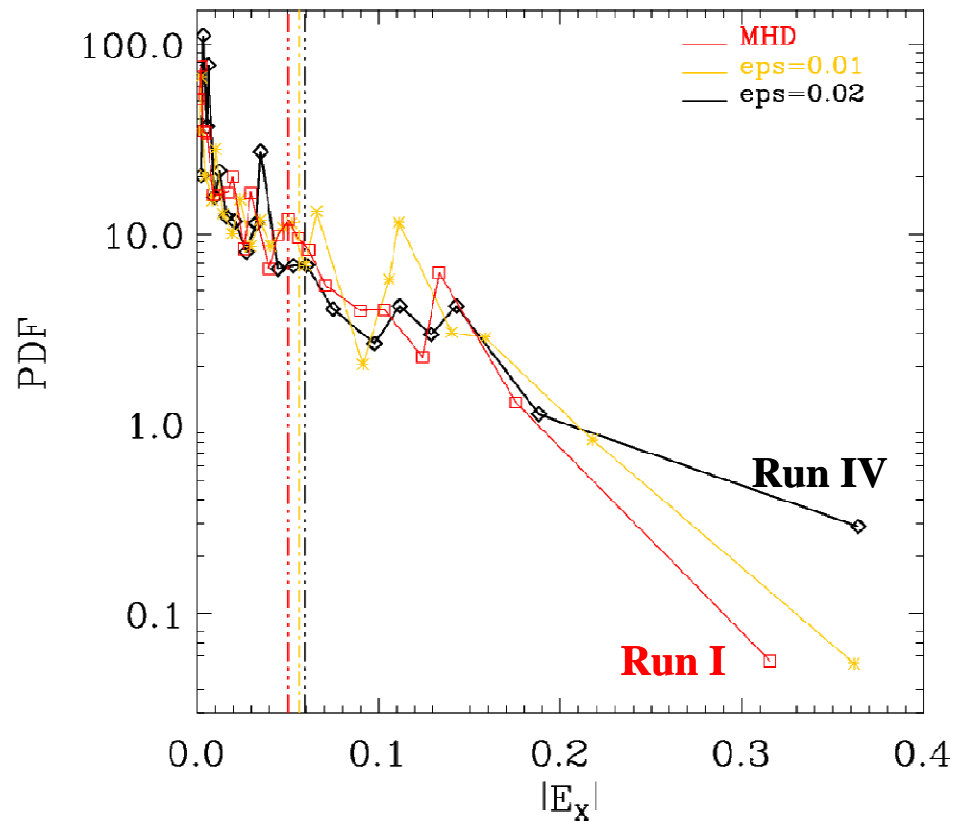
#reconnection events/
#reconnection zones

number of identified TD
events as a function of the
threshold, normalized by
the value at $\theta=1$

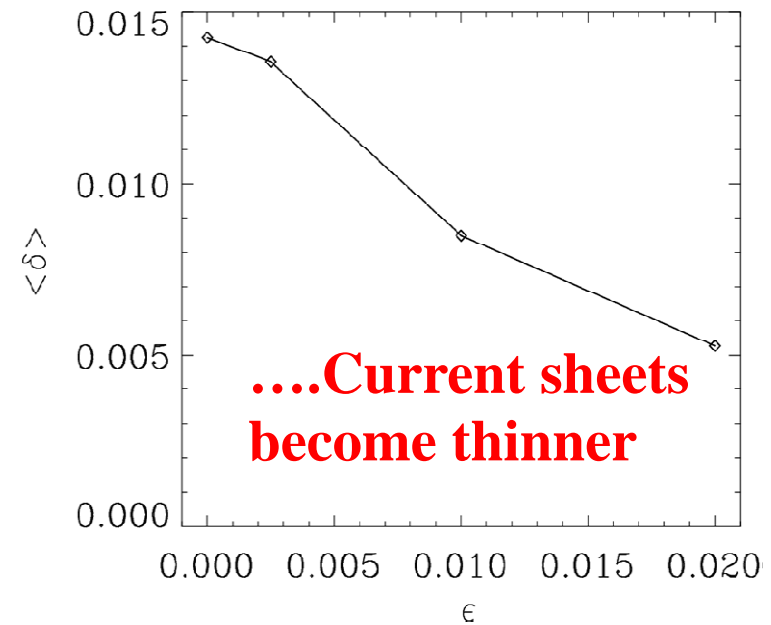
Servidio et al. , JGR 2011

**Strongest discontinuities are
reconnection events**

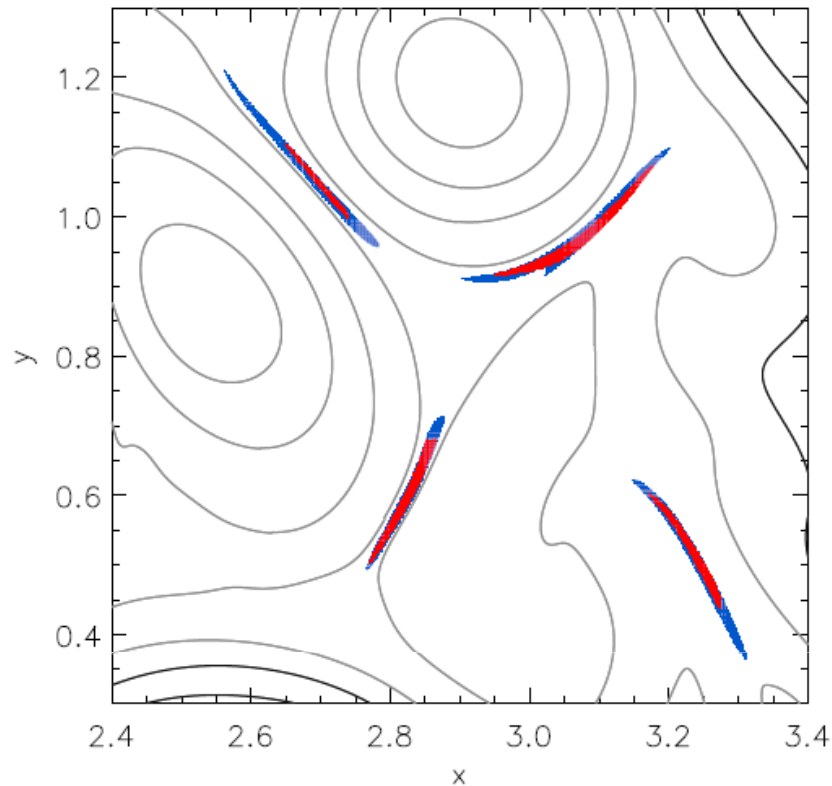
Reconnection in Hall MHD Turbulence



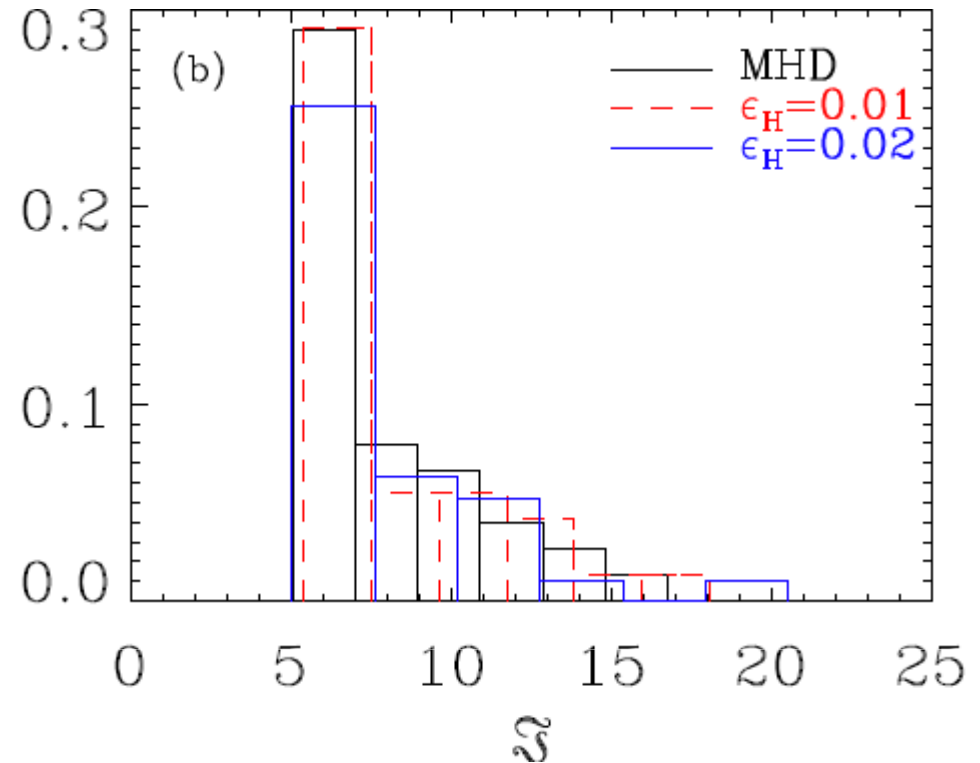
Run	ϵ_H
I	0.0 (MHD)
II	0.0025
III	0.01
IV	0.02



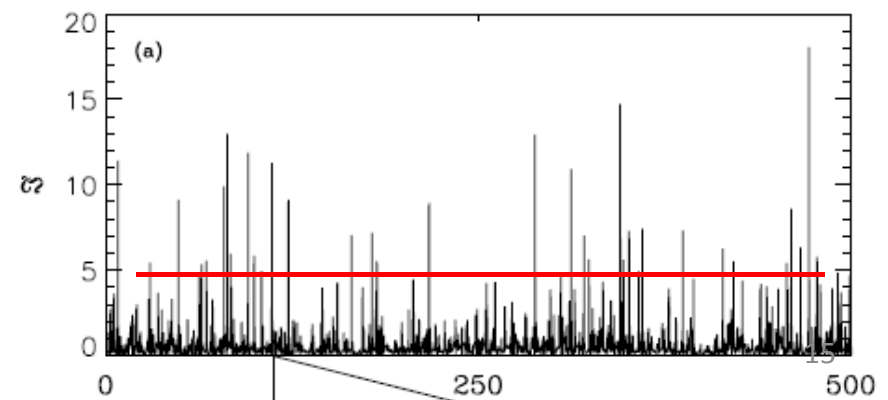
The Hall electric field increases the reconnection rate in turbulence, but...



Contour lines of the in-plane magnetic field together with the diffusion regions in a sub-regions of the simulation box from a MHD simulation (blue shaded map) and from an HMHD one (red shaded map)



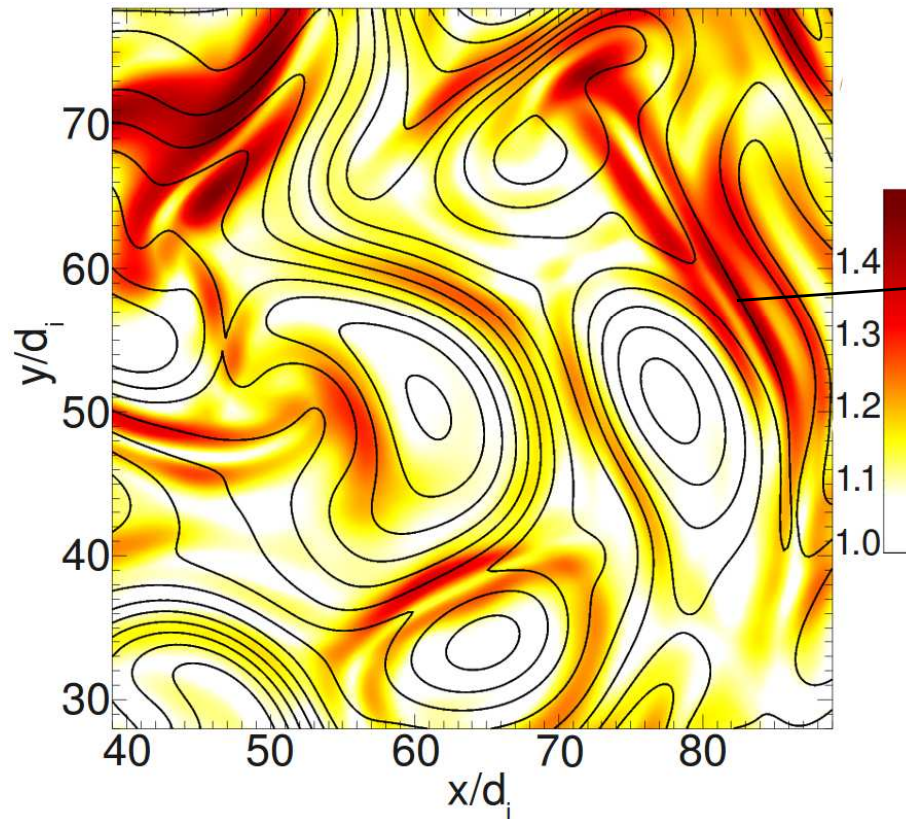
Distribution functions of the PVI signal peaks across the current sheets using a threshold $\theta = 5$ and for $\epsilon = 0, 0.01, 0.02$



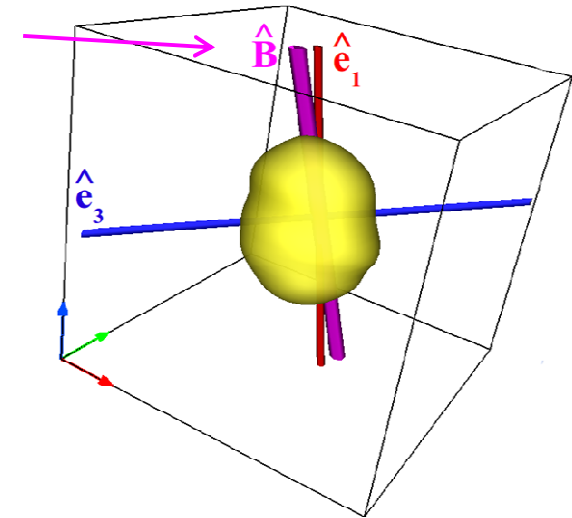
• Distribution Functions near Reconnection Zones

Vlasov simulation of a 2D turbulence (*Valentini et al.*, PRL 2010)

From *Servidio et al.*, PRL 2012 the main result was that kinetic effects are non-homogeneous: anisotropy is localized in spatial patches



Local magnetic field



the DF is strongly affected by turbulence, resembling an elongated potato-like structure

Anisotropy is higher in snake-like streams of strong magnetic stress, current sheets, magnetic field jets, and reconnection

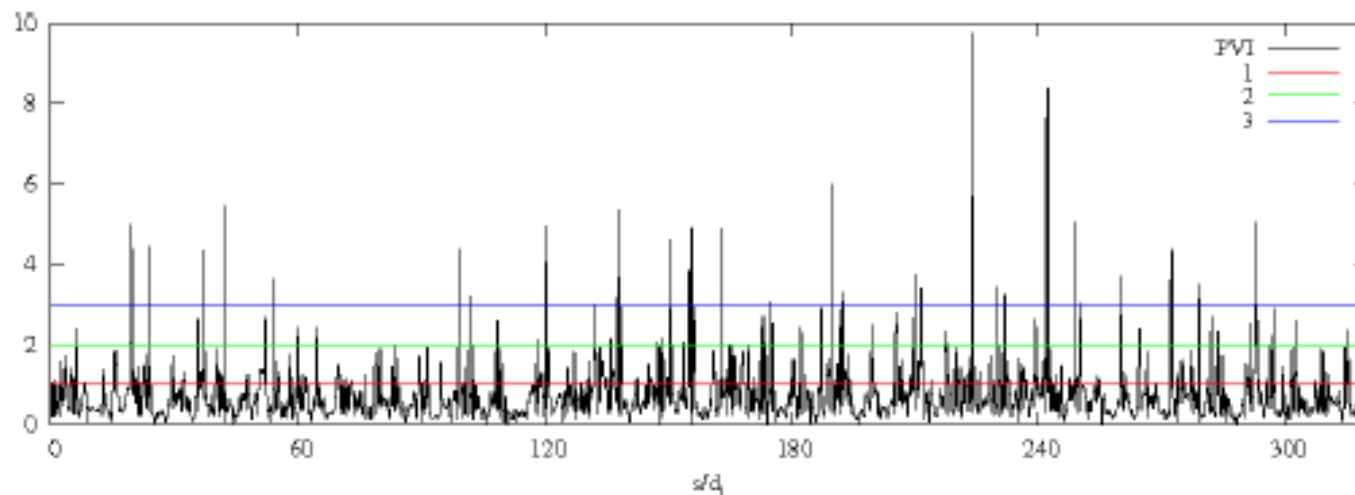
A more general estimate of the non-Maxwellian behavior of the plasma is given by

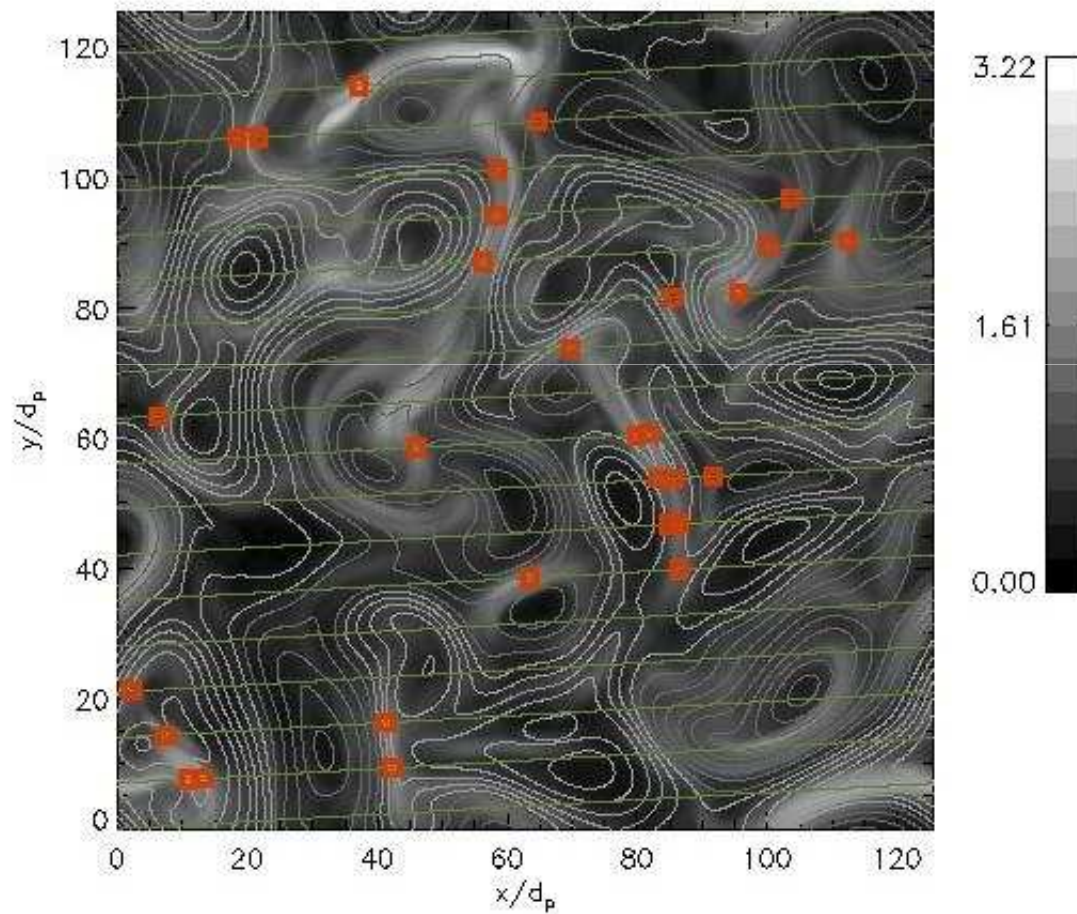
$$\epsilon(x, y) = \frac{1}{n} \sqrt{\int (f - g)^2 d^3v}$$

where g is the associated Maxwellian distribution computed from the parameters of f

ϵ describes non-Maxwellian features, like, for example, temperature anisotropy, non-zero skewness (heat flux), or high (low) kurtosis

We adopt a spacecraft – like sampling and we fix our attention on the structures it samples





Shaded contour of the function ε (%), together with the magnetic field lines. The one-dimensional path s is in green line.

The discontinuities identified by PVI technique with a threshold $\theta = 3$ are the red open squares.

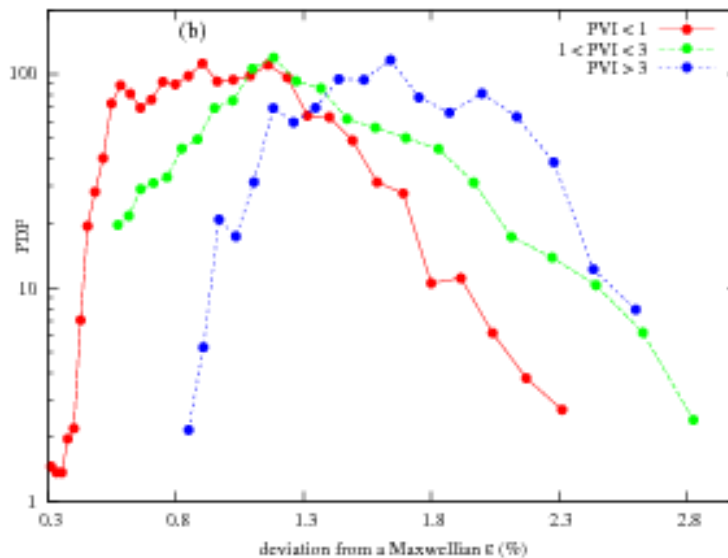
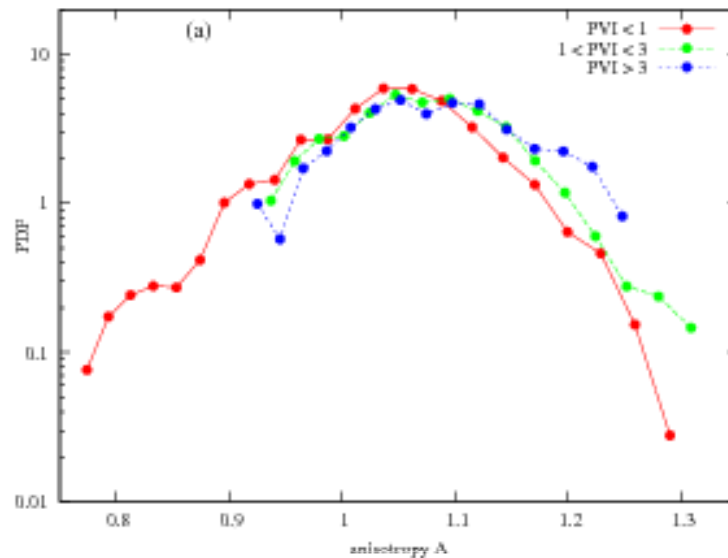
Regions of high kinetic effects are mostly concentrated near magnetic discontinuities
(*Greco et al.*, in preparation)

A and ε can be grouped according to which the PVI values they correspond to:

$PVI < 1$ corresponds to low value fluctuations

$1 < PVI < 3$ removes low value fluctuations and retains the non- Gaussian structures

$PVI > 3$ contains only most highly inhomogeneous structures including current sheets



The largest and most important distortions of the proton distribution function occur in the immediate vicinity of discontinuities and not in the smoothest regions.

The two panels also suggests that there exists a hierarchy of current sheet intensities, where the most intense are associated with the most non-homogeneous kinetic effects

(as recently shown in solar wind, see *Osman et al.*, PRL 2012)

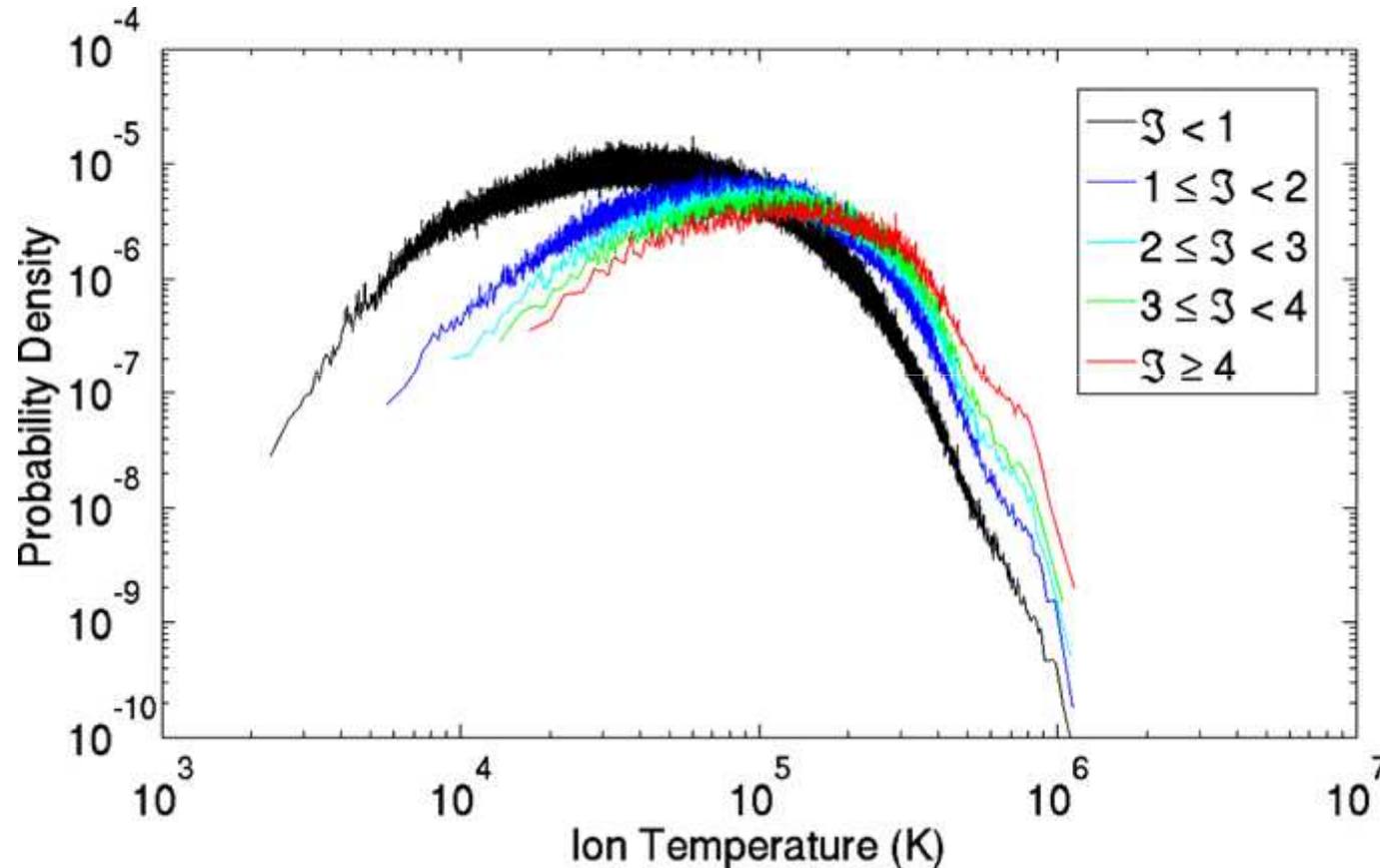
By this time we know that PVI-threshold methods perform well to find non-Gaussian tails, coherent structures, many of which are current sheets, and at higher thresholds, reconnection sites, where the most important non-Maxwellian features of the DF are concentrated

With the exception of the last point, the earlier works have been kinematic in nature.

More recently works have shown a new direction for PVI methods that is helping to understand dynamical processes, including dissipation and heating

Solar wind proton temperature distributions conditioned on PVI

Most intense current sheets are associated with largest heating



Similar effects in:

- electron Temp
- electron heat flux

Wind s/c Data

Osman et al., ApJ 2011

$$PVI = \frac{|\Delta \mathbf{B}|}{\sqrt{\langle |\Delta \mathbf{B}|^2 \rangle}}$$

PDFs of the ion temperature, where each PDF corresponds to a different range of PVI. As the PVI values increase, the probability density decreases at lower temperatures and increases at higher temperatures. Also, the mean ion temperature increases with increasing PVI.

Plasma with the greatest proportion of intense coherent structures has the highest most probable parallel and perpendicular temperatures.

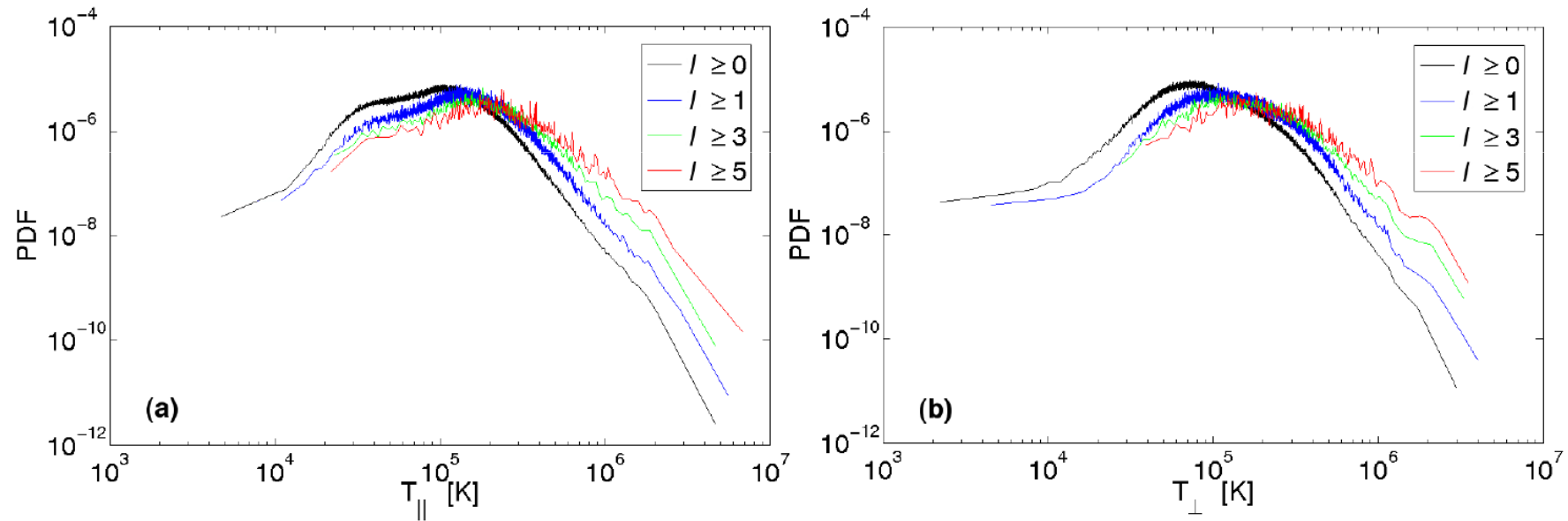
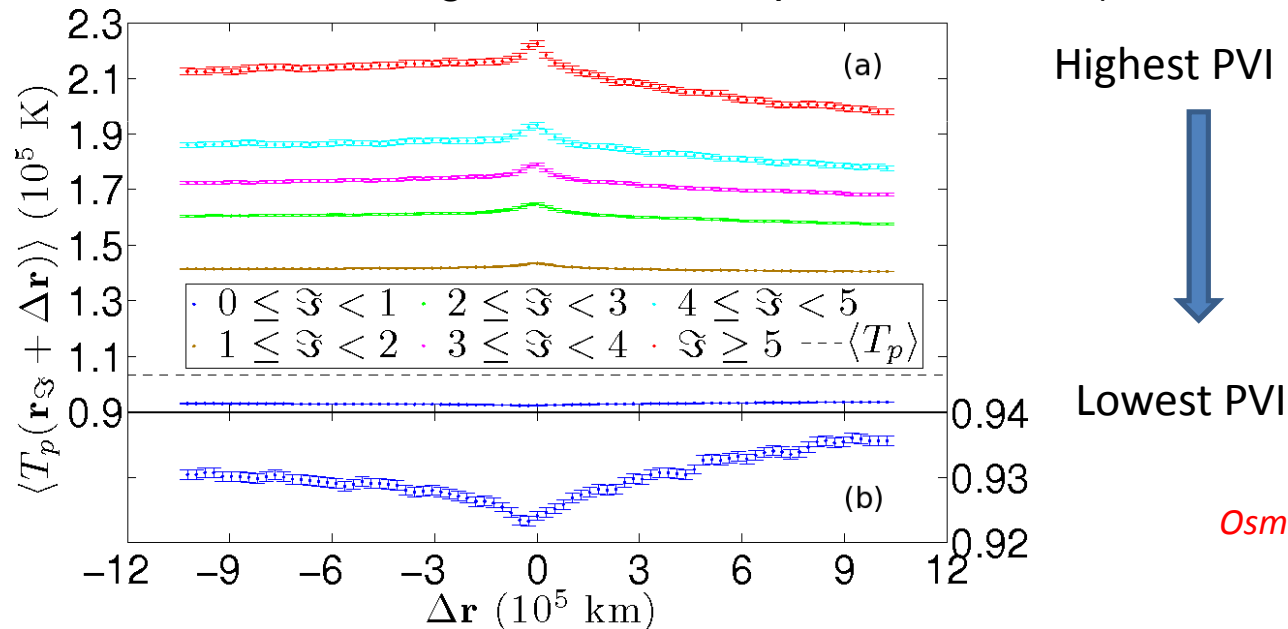


FIG. 3. PDFs of the (a) parallel and (b) perpendicular proton temperatures, where each corresponds to a different range of PVI values. In both cases, the strongest PVI events are associated with elevations in temperature.

Local Structure of temperature near current sheets

This heating appears in anisotropic proportions in the vicinity of the most non-Gaussian structures. Therefore, this suggest the presence of dynamical heating mechanisms within or nearby these coherent structures that can heat and accelerate protons both parallel and perpendicular to the magnetic field direction.

- Temperature profile around a coherent structure:
(entire ACE 64 sec magnetic field and plasma dataset).



Osman et al., PRL 2012

- Mean proton temperature LOWEST in the most uniform samples (low PVI)

Temperature anisotropy and elevated plasma beta are found to be statistically associated with measures of coherent magnetic structures

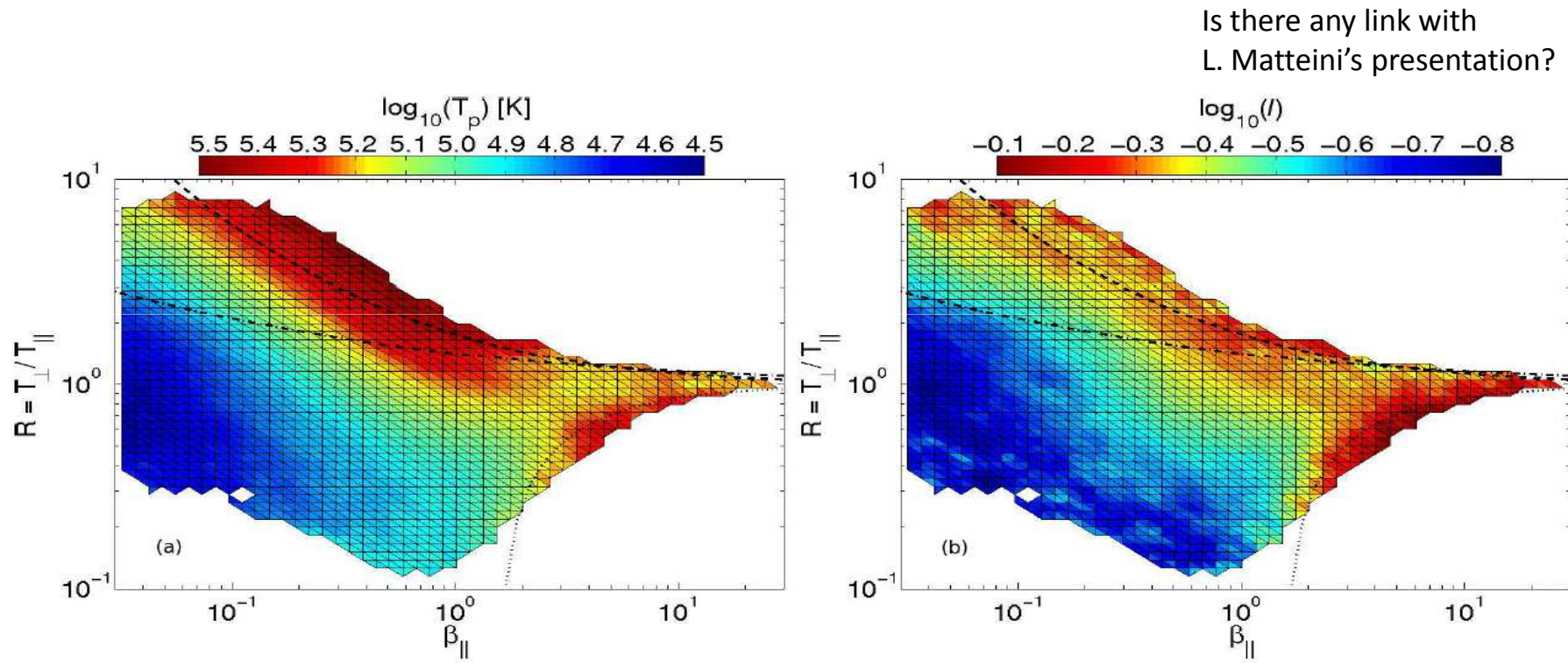


FIG. 1. Plot of median (a) scalar proton temperature T_p , and (b) PVI statistic I over the $(\beta_{\parallel}, T_{\perp}/T_{\parallel})$ -plane. The curves indicate theoretical growth rates for the mirror (dashed), cyclotron (dot-dashed), and oblique firehose (dotted) instabilities. There is a manifest association between these thresholds, hot plasma, and enhanced PVI.

Is the solar wind an *active turbulent medium*?

Do the statistical signatures of coherent structures evolve with heliocentric distance in the inner heliosphere, in analogy ,e.g., to the evolution of the breakpoint?

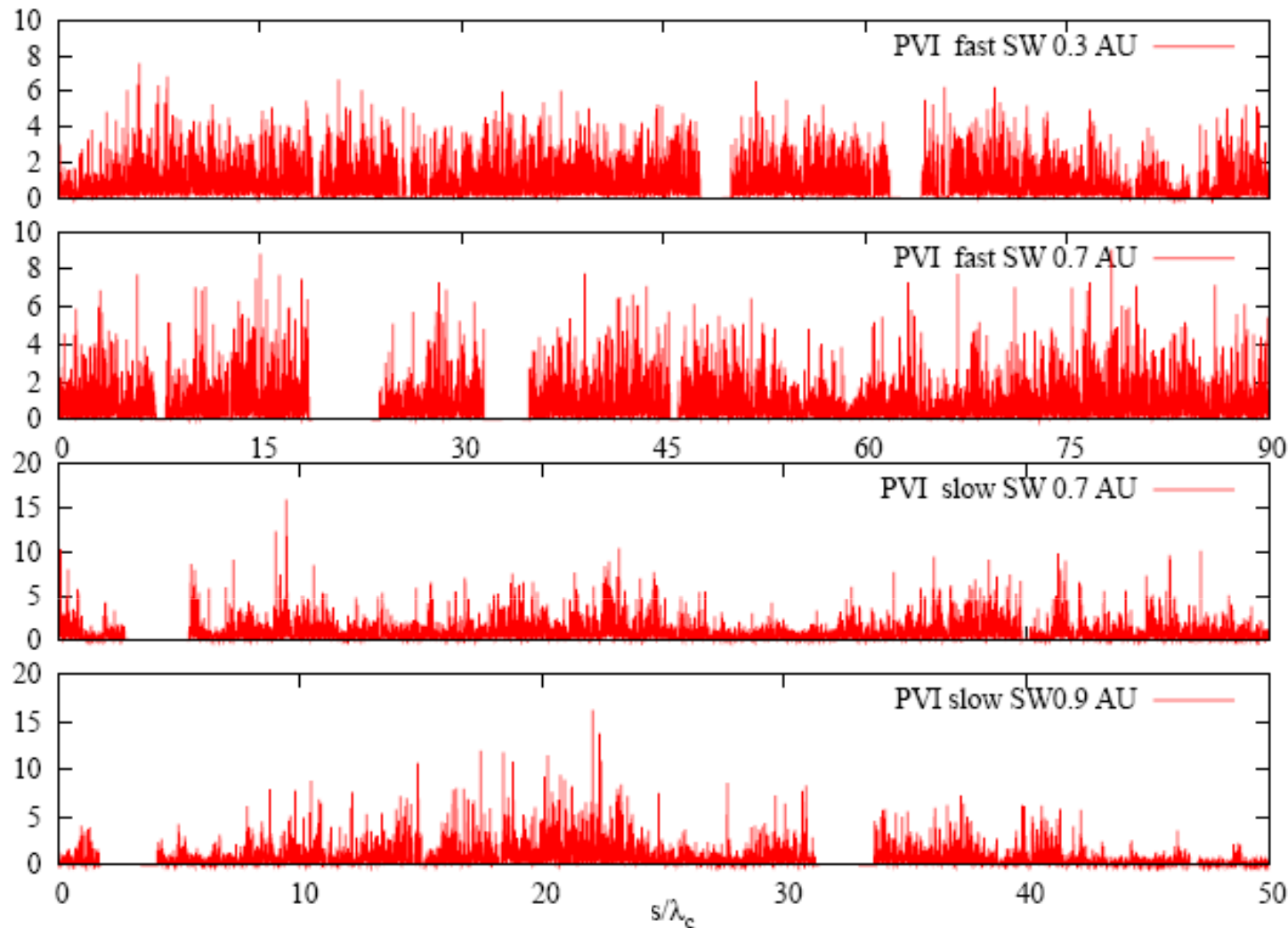
The only available dataset that can address the questions on the evolution of the intermittent structures in the inner heliosphere, is data from the Helios mission.

The present data analysis is based on 6 s averages of magnetic field recorded by the Rome/GSFC magnetometer on Helios 2 during its primary mission to the Sun in 1976.

time interval [ddd:hh - ddd:hh]	radial distance [AU]	$\langle V \rangle$ [km/s]	convective age [h]	No. of points
49:14 - 51:14	0.88	643	57	28800
75:12 - 77:12	0.65	630	43	28800
105:12 - 107:12	0.29	729	16.6	28800
46:00 - 48:00	0.9	433	86.6	28794
72:00 - 74:00	0.7	412	70.8	27943
99:12 - 101:12	0.3	405	30.9	28800

Greco et al., ApJ 2012

Convective age = $R / \langle |V| \rangle$ is the clock time since leaving the sun²⁵



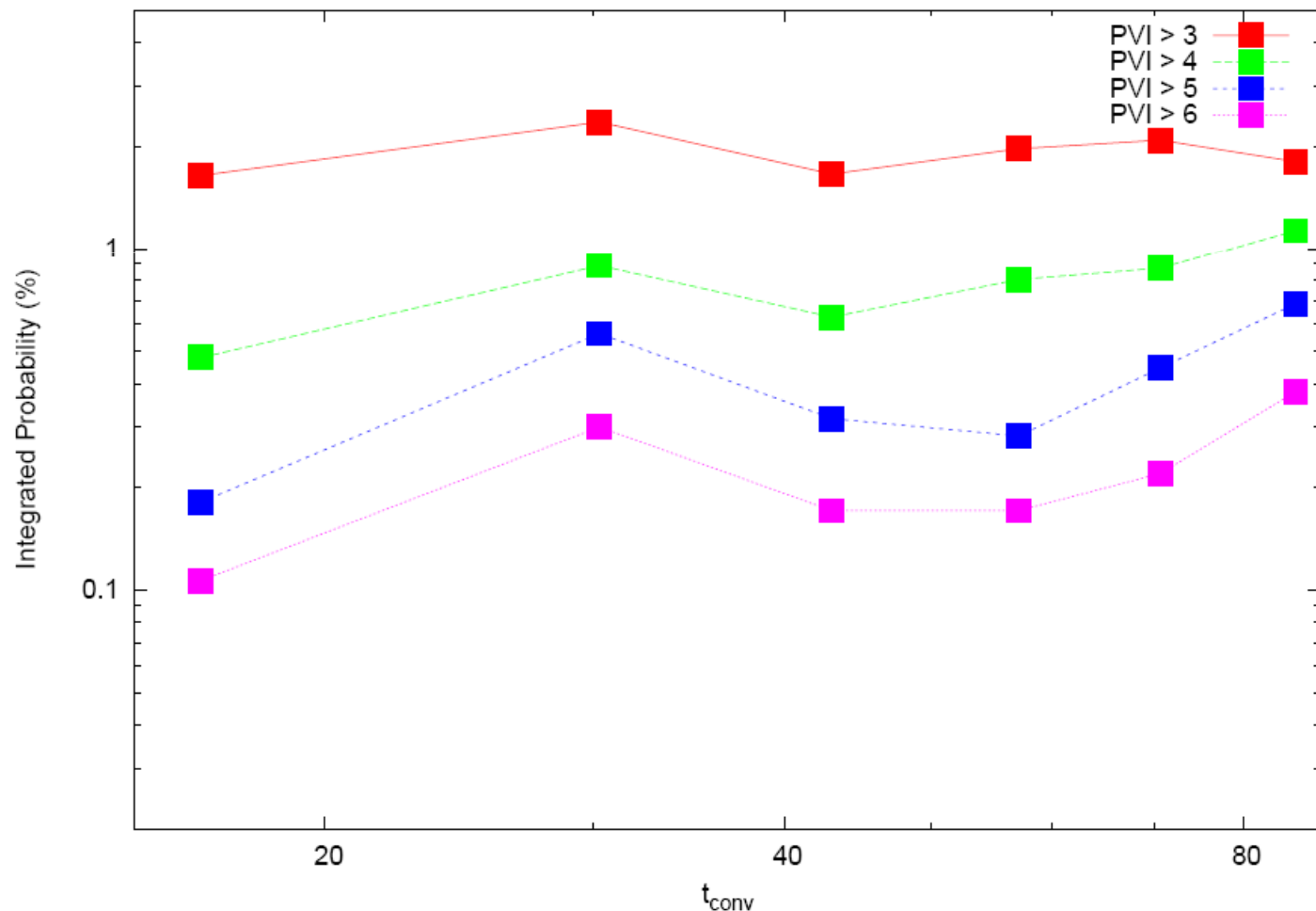
Time/space series of PVI computed for some of the six streams from solar wind by Helios 2. Space is normalized to the correlation scale, using frozen-in flow.

$$\lambda_c = 1.2 \times 10^6 \text{ km}$$

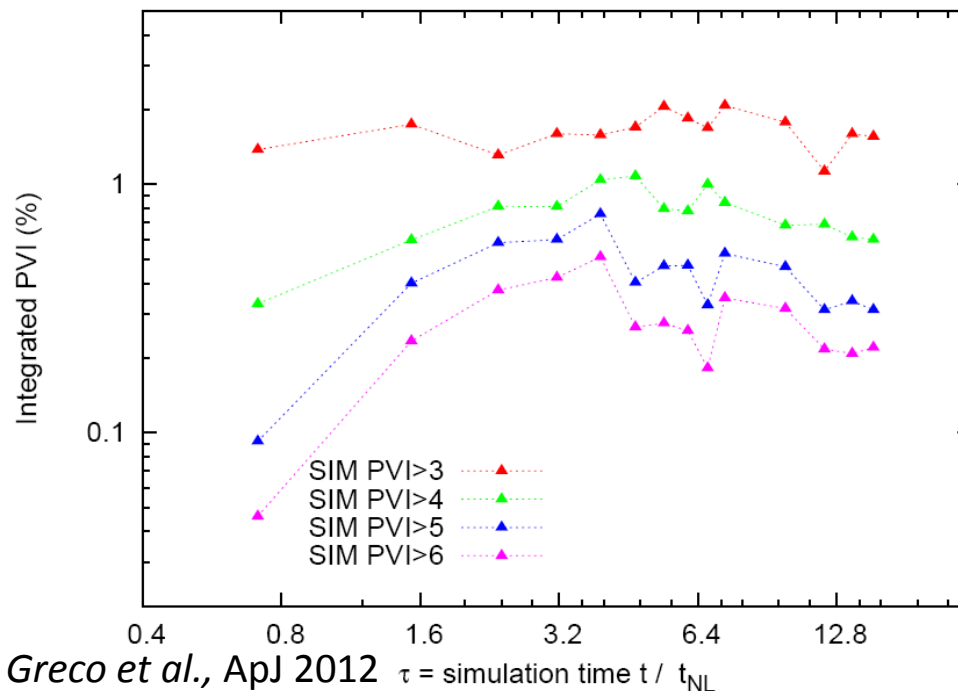
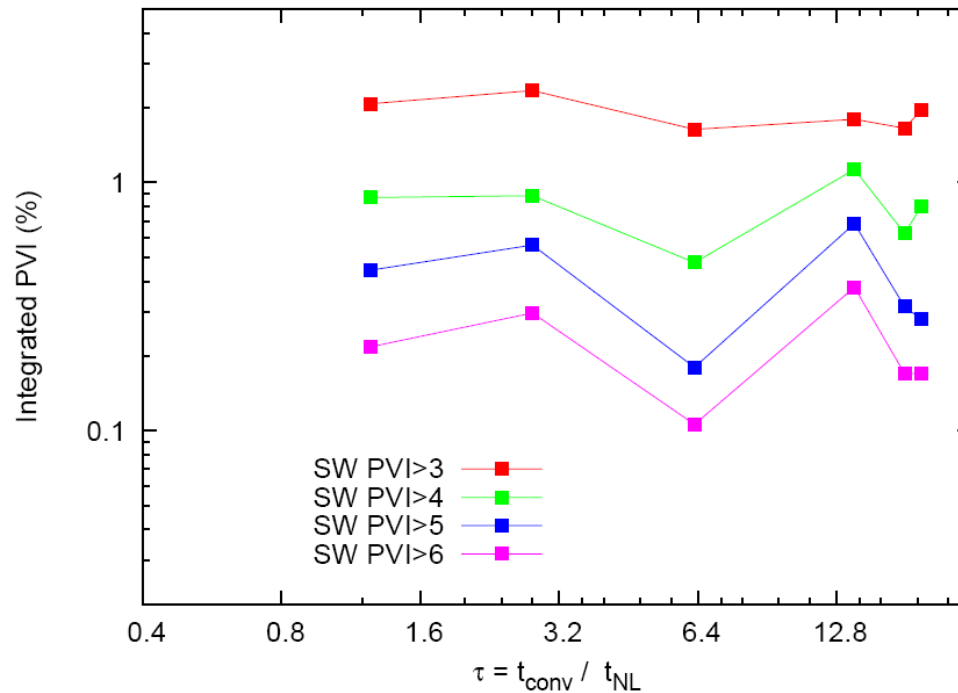
$$\Delta s = 0.004 \lambda_c$$

PVI series show the typical behavior of an intermittent signal, with bursty spikes due to sharp gradients of the magnetic field and related to the presence of structures at smaller separations.

We compute the cumulative probability of finding the PVI signal above a specified threshold. This can be interpreted as the fractional volume occupied by the current sheets. The higher the cumulative probability, the greater is the density of strong discontinuities present.



The plots, especially for higher cutoff, shows clear trend upwards with the convective age. This may indicate that the turbulence is developing more strongly intermittent events as the wind ages while propagating away the Sun.



The graphs corresponding to the same cutoff have the same trend.

Those corresponding to “PVI> 3” do not show large variations with τ . On the contrary, the plots corresponding to “PVI> 6” display a rich behaviour in function of the dimensionless age.

Clearly, we have much less points in the solar wind data set, but from the comparison with the simulation case, we can extrapolate the behaviour of the solar wind and say that the likelihood of finding coherent structures increases substantially up to 2 – 3 nonlinear times, then we can observe a sort of decrease and then a saturation.

In any case, a clear development of intermittency is present as the turbulence ages, indicating that coherent structures are not passively advected but are themselves an integral part of the turbulent cascade.

A “simple” sketch

